Low Cycle Fatigue Criteria for Mild Steel Bars under Combined Bending and Axial Loading

Rami Hawileh[1], Adeeb Rahman[2], Habib Tabatabai[3]

University of Wisconsin-Milwaukee
Dept. of Civil Engineering and Mechanics, P.O.Box 784, Milwaukee,WI 53211
[1] PhD Candidate. rhawileh@uwm.edu. [2] Assistant Professor. [3] Associate Professor.

Nomenclature

R = radius of curvature
$d\theta$ = angle of rotation
ε_b = maximum bending strain
d_b = bar diameter
η_{des} = distance from the compression face of the beam to the neutral axis at θ_{des} divided by the height of the beam
ζ = distance from the center of the mild steel bar to the nearest face divided by the height of the beam
h_g = beam height
θ_{des} = maximum (design) interface rotation
L_{su} = unbonded length of the mild steel bar at each interface

ε_{ap} = plastic strain amplitude = $\frac{\varepsilon_{p,max} - \varepsilon_{p,min}}{2}$

ε_{bp} = plastic bending strain amplitude = $\frac{\varepsilon_{b,max} - \varepsilon_{b,min}}{2}$

$\Delta\varepsilon_p$ = range of plastic strain = $\varepsilon_{p,max} - \varepsilon_{p,min}$

$\Delta\varepsilon_b$ = range of bending plastic strain = $\varepsilon_{b,max} - \varepsilon_{b,min}$

$\varepsilon_{p,max}$ = maximum plastic strain in a cycle

$\varepsilon_{b,max}$ = maximum bending plastic strain in a cycle

$\varepsilon_{p,min}$ = minimum plastic strain in a cycle

$\varepsilon_{b,min}$ = minimum bending plastic strain in a cycle

N_f = number of cycles to failure

ABSTRACT

While a low cycle fatigue criteria is well established for mild steel bars under axial loading, the effect of combined axial and bending loading is not fully developed experimentally nor analytically. This paper intends to address this condition that is applicable to the behavior of mild steel bars in a hybrid frame design. The behavior of mild steel plays a significant role in the behavior of prestressed precast hybrid frames. They were used in the PRESSS program [8] to prevent potential collapse of buildings erected using hybrid frames. The mild steel is expected to undergo yielding and large deformation to absorb snd dissipate energy in an earthquake event. A non-linear finite element analysis of a 3-D model of a hybrid frame [Hawileh, 2003], shows that mild steel bars, designed to dissipate energy, exhibit significant inelastic axial and bending strains under cyclic loading. This prompted a need for considering the low cycle fatigue life for the mild steel bars under bending and axial loading. The FE model shows the potential vulnerability of mild steel bars to low cycle fatigue failure. The bar could potentially be subjected to failure due to low cycle fatigue limiting its usefulness to dissipate energy in earthquake loading.

A mild steel fracture criterion is therefore needed in the design procedure for hybrid frame by controlling the total plastic strains in the mild steel bar below a maximum limit. This paper will present analytical derivation to account for development of two equations one which predict the axial strain ε_{axial} and one for the bending strain ε_b both in

the plastic range. The total of the two strains will be compared to the allowable strain proposed by Mander [4] to predict the fatigue life of the bar.

INTRODUCTION

From preliminary nonlinear FEA analyses of a 3-D model of a hybrid frame system [Hawileh, 2004], it was determined that the mild steel bars in a hybrid frame exhibit significant inelastic axial and bending strains more than their intended design. Once the gap at the beam-column interface opens, relatively high levels of repetitive plastic strains develop in the mild steel bars. This prompted a need for considering the low-cycle fatigue of the mild steel bars including both bending and axial strains. The relatively high inelastic strains in the FE model show the potential vulnerability of mild steel bars to low-cycle fatigue failure. It should be noted that both the PRESSS [Stanton and Nakaki, 2002] and National Institute of Standards and Technology (NIST) [Cheok and Stone, 1994] test reports indicate bar fractures during cyclic testing.
A mild steel fracture criterion is therefore needed in the design procedure for hybrid frames by controlling the total plastic strains in the mild steel bar below a maximum value. This criterion should be based on the low-cycle fatigue behavior of reinforcing steel.

Mander and Panthaki (1994) studied the behavior of reinforcing steel bars under low-cycle fatigue subjected to axial-strain reversals with strain amplitudes ranging from yield to 6%. Liu (2001) studied the low-cycle fatigue behavior of steel bars subjected to bending strain reversals with variable amplitudes. In this study, a mild steel fracture criterion under combined axial and bending strains is proposed based on the works of Mander, Panthaki, and Liu.

Low-Cycle Fatigue for Bar Fracture

Mander (1994) experimentally evaluated the low-cycle fatigue behavior of reinforcing steel bars subjected to cyclic axial strain amplitudes ranging from yield to 6%. He also evaluated the experimental results with low-cycle fatigue models found in the literature. His experimental data were fit to existing fatigue equations. As a result, low-cycle fatigue life relationships were developed for reinforcing steel bars. The relationship between plastic-strain amplitude (ε_{ap}) and low cycle fatigue life for axial deformations of A615 steel bars developed by Mander is as follows:

$$\varepsilon_{ap} = \frac{\Delta\varepsilon}{2} = 0.0795(2N_f)^{-0.448} \quad (1)$$

We will use this equation as a fatigue criterion to examine the equation we will develop in this paper as follows:

$$\varepsilon_{total} = \varepsilon_{axial} + \varepsilon_b \le \varepsilon_{ap} \quad (2)$$

In the design of hybrid frame connection, the unbonded length of the mild steel bar L_{su} is needed to limit low cycle fatigue in the bar. The ε_{axial} will be calculated from ε_{ap} - ε_b. This will allow designers to find the safe unbonded length L_{su} of the mild steel bar at the beam-column interface.

Bending Strain Calculations for Bars

Liu (2001) presented the following procedure for calculating strain-displacement relationships for bars subjected to bending when the material is stressed beyond the elastic range. Consider the deformed bar segment shown in Figure 1 below.

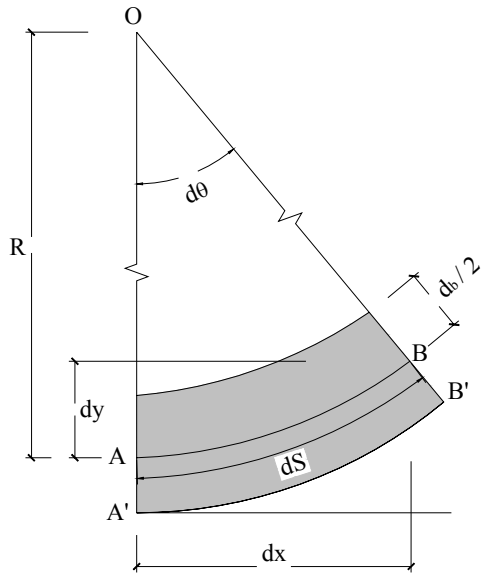

Figure 1: Deformed Segment of Mild Steel Bar

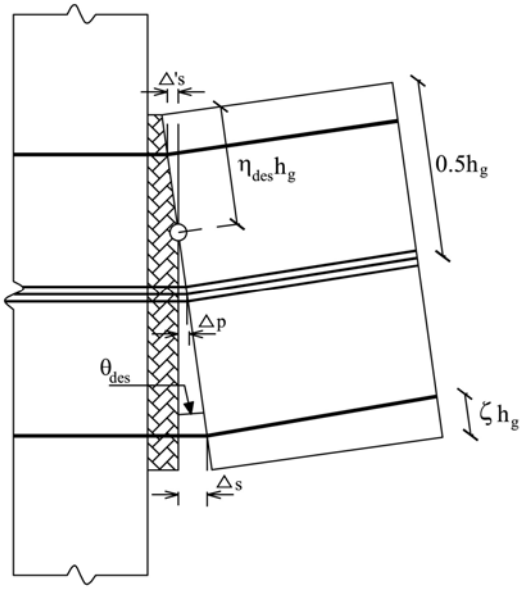

Figure 2: Location of the Center of Rotation at θ_{des} (Stanton and Nakaki, 2002)

Assuming that the cross section of bar is symmetric (i.e. elastic and plastic neutral axes are at the center of the bar), the bending strain and the radius of curvature can be calculated as follows:

$$\varepsilon_b = \frac{A'B' - ds}{ds} = \frac{\left(R + \frac{d_b}{2}\right)d\theta - R\,d\theta}{R\,d\theta} = \frac{d_b}{2}\left(\frac{1}{\mathrm{R}}\right) \tag{3}$$

$$\frac{1}{R} = \frac{\frac{y''}{1+y'^2}dx}{dx\left(1+y'^2\right)^{1/2}} \tag{4}$$

Axial Strain Calculations for Bars

In Figure 3 shown below, the solid line CD is the initial unbonded length of the reinforcing bar in a hybrid frame. The dashed line DE shows the path that the end D of the unbonded segment of the mild steel bar would take as it moves from D to E.

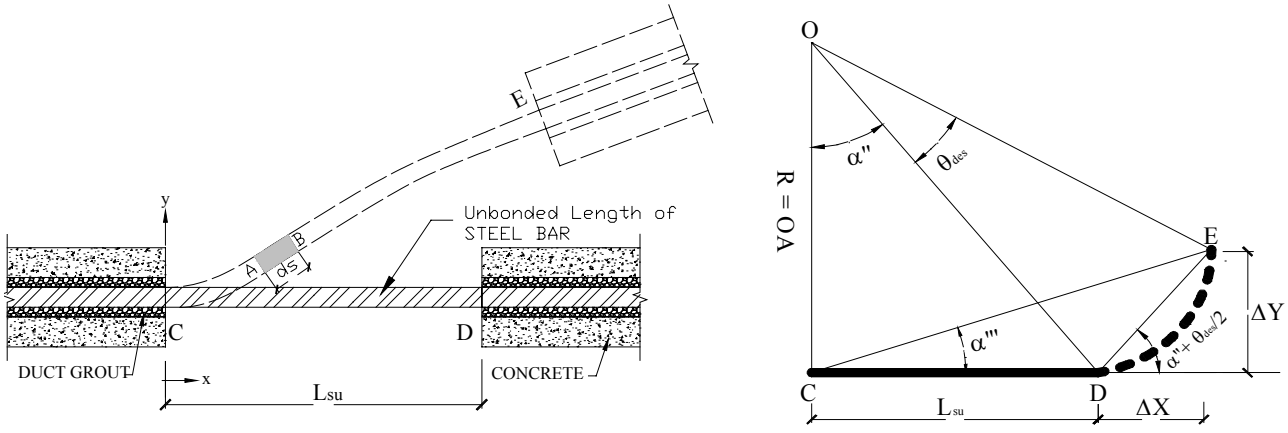

Figure 2: Path of point D of the unbonded segment of the mild steel bar

Assuming that the center of rotation ″O″ shown in Figure 1 for the opening of the joint at the beam-column interface is at the neutral axis of the beam when the hybrid frame is subjected to a design interface rotation of θ_{des}, the following can be written using the same assumptions as in PRESSS program (Figure 2 and 3).

$$R = (1-\zeta-\eta_{des})h_g \tag{5}$$

$$\& \ \varepsilon_{a,a} = \frac{\Delta s}{L_{su}} \tag{6}$$

Where Δs is the horizontal gap opening at the location of the tension bar at the beam-column interface (Figure 3) and $\varepsilon_{a,a}$ is the axial bar strain as calculated in the PRESSS program assuming that there is no vertical movement at the end of the bar as a result of rotation. The Δs and L_{su} can be written as:

$$\Delta s = R\theta_{des} = h_g(1-\zeta-\eta_{des})\theta_{des} \tag{7}$$

$$L_{su} = \frac{\Delta s}{\varepsilon_{a,a}} = \frac{\theta_{des}h_g(1-\zeta-\eta_{des})}{\varepsilon_{a,a}} \tag{8}$$

However,

$$\Delta X = \frac{(1-\eta_{des}-\zeta)h_g\theta_{des}}{\varepsilon_{a,a}}\left(\theta^2{}_{des}+\varepsilon^2{}_{a,a}\right)^{\frac{1}{2}}\cos\left(\frac{\theta_{des}}{2}+\alpha''\right) \tag{9}$$

$$\Delta Y = \frac{(1-\eta_{des}-\zeta)h_g\theta_{des}}{\varepsilon_{a,a}}\left(\theta^2{}_{des}+\varepsilon^2{}_{a,a}\right)^{\frac{1}{2}}\sin\left(\frac{\theta_{des}}{2}+\alpha''\right) \tag{10}$$

The axial strain in the reinforcing bar (ε_{axial}) can be written as:

$$\varepsilon_{axial} = \frac{\sqrt{(L_{su}+\Delta X)^2+\Delta Y^2}-L_{su}}{L_{su}} \tag{11}$$

$$\boldsymbol{\varepsilon_{axial} = \left[1+2\left(\theta^2{}_{des}+\varepsilon^2{}_{a,a}\right)^{\frac{1}{2}}\cos\left(\frac{\theta_{des}}{2}+\alpha''\right)+\left(\theta^2{}_{des}+\varepsilon^2{}_{a,a}\right)\right]^{\frac{1}{2}}-1} \tag{12}$$

Inelastically Deformed Geometry of Bars

A FE model can be used to accurately predict the inelastically deformed shape of the bar. Once an equation for the deflected shape of the bar is derived, the bending and axial strains of the bar can be calculated using equations 1 and 10.

A parametric study involving multiple nonlinear FE models was performed to understand the combined axial and bending behavior of the mild steel bar for six different cases listed in Table 1 below.

Table 2.1 Study Cases

No.	$(1-\eta_{des}-\zeta)h$	θ_{des}	L_{su} (inches)	α'' (rad.)	ΔX (inches)	ΔY (inches)	$\Delta X/L_{su}$
1	20	0.02	10	0.4636	0.398	0.204	0.0398
2	20	0.04	20	0.7854	0.784	0.816	0.0392
3	30	0.02	15	0.4636	0.597	0.306	0.0398
4	30	0.04	30	0.7854	1.176	1.224	0.0392
5	20	0.01	5	0.245	0.200	0.051	0.04
6	20	0.02	20	0.7854	0.396	0.404	0.0198

The FE Model

The undeformed geometry of the mild steel bar at the beam-column interface is modeled as shown in Figure 4 and Table 2 below. The partially unbonded bar and two concrete blocks representing parts of the beam and column are modeled. The length of the concrete block is assumed to be 20 inches on each side of the unbonded length of the bar to provide sufficient bar bonded length for all study cases.

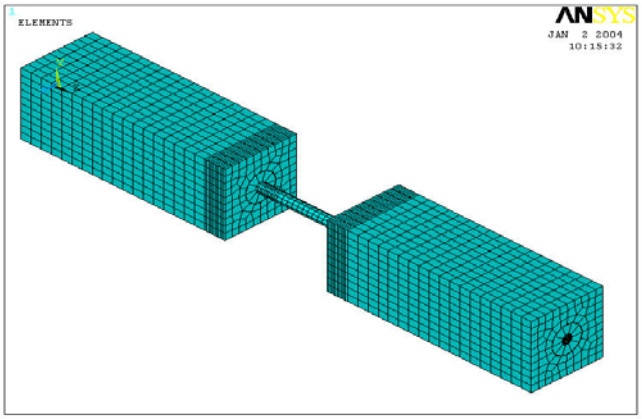

Table 2: Model Dimensions

Material	Width (in)	Height (in)	Diameter (in)	Area (in^2)
Bar	_	_	1	0.785
Grout	_	_	3	6.281
Concrete Block	7	7	_	41.932

Figure 4: Isoparametric View of the entire Model

The ANSYS finite element program was utilized [ANSYS user manual, version 7.1, 2000]. BEAM188 element is used to model the entire model. The element has six degrees of freedom at each node. The degrees of freedom at each node include translations in x, y, and z directions, and rotations about the x, y, and z directions. BEAM188 has linear, large rotation, and/or large strain nonlinear capabilities. The most important characteristic of BEAM188 is that it can be used with any cross section. Elasticity and plasticity models are supported (irrespective of cross section subtype). This element is based on the Timoshenko beam theory [1]. Shear deformation effects are also included.

Material Properties

Figures 5 and 6 below show the stress strain diagrams for the mild steel bar and concrete. The modulus of elasticity used in the model is 4900 ksi for concrete, 29,000 ksi for steel, and 3500 ksi for the duct grout.

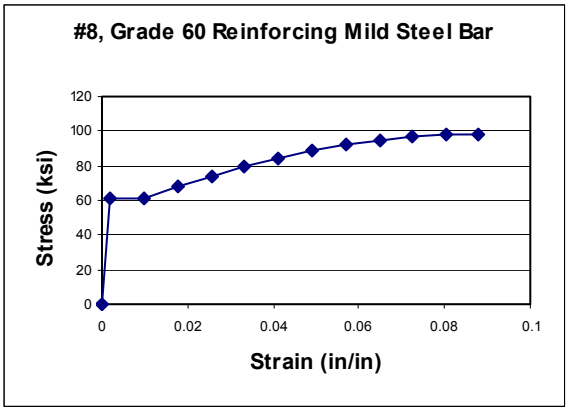

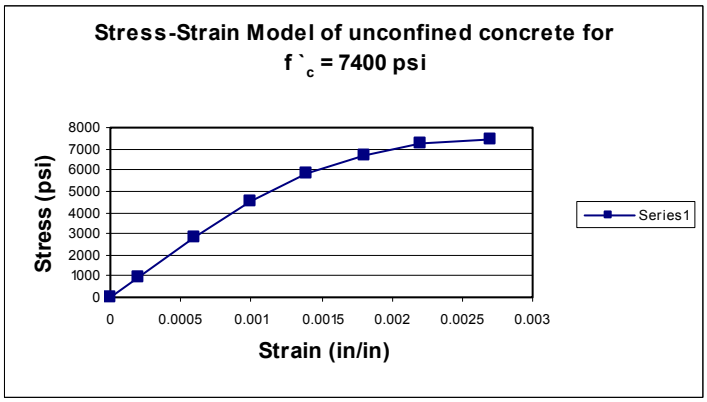

Figure 5: Stress-Strain Curve of Steel Bar [8] Figure 6: Stress-Strain Model of Concrete [9]

The densities of steel (mild steel and post-tensioning) and concrete were assumed to be 490 lb/ft^3 and 150 lb/ft^3, respectively. The Poisson's Ratio (ν) was assumed to be 0.3 for steel and 0.2 for concrete.

Boundary Conditions and Loads

The entire concrete block nodes on the left side of the bar's unbonded length were restrained (fixed) in all 6 directions (Figure 4). All of the concrete block nodes at the right end of the unbonded mild steel bar were simultaneously deformed to achieve the following concurrent displacements and rotation: A horizontal displacement ΔX; a vertical displacement ΔY; and a rotation θ_{des}. The grout and reinforcing bar elements were not restrained in either block. The values of these applied displacements for the six different cases are listed in Table 1. The relative magnitudes of these displacements are consistent with the deformations in hybrid frames.

Results and Conclusions

The FE model provides full fields of stress and strain throughout the model. Figure 7 shows the deflected shape of the entire model. Figures 8 and 9 show the horizontal and vertical deformations for Model No. 1. The total (elastic + plastic) axial strains and stresses for bar is shown in Figure 10. The results for the bar axial and bending strains are listed in Table 3.

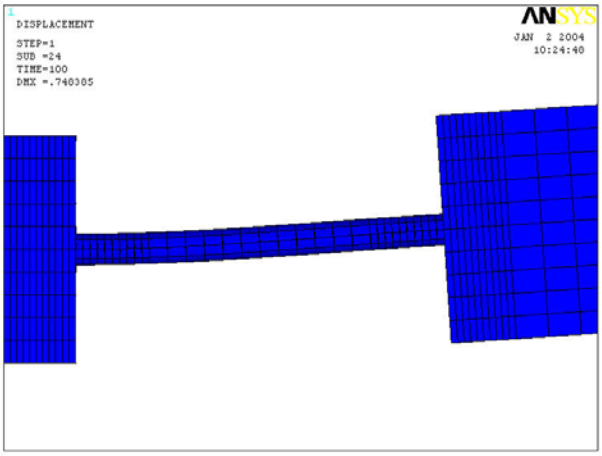

Figure 7: Deflected Shape of the Model

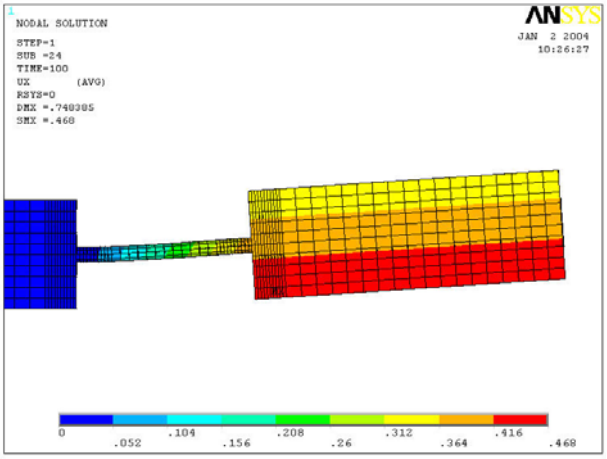

Figure 8: Horizontal Deformation of the Model

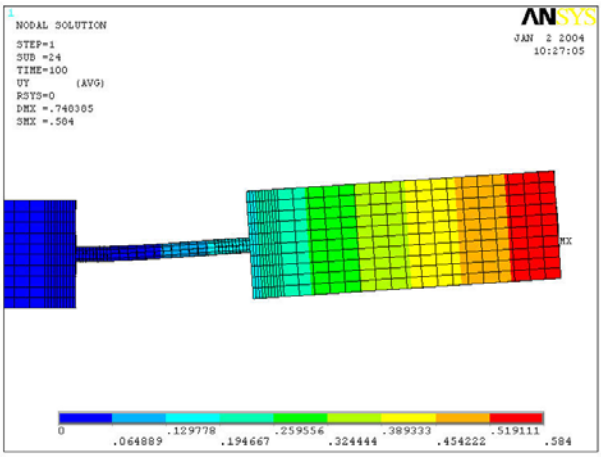

Figure 9: Vertical Deformation of the Model

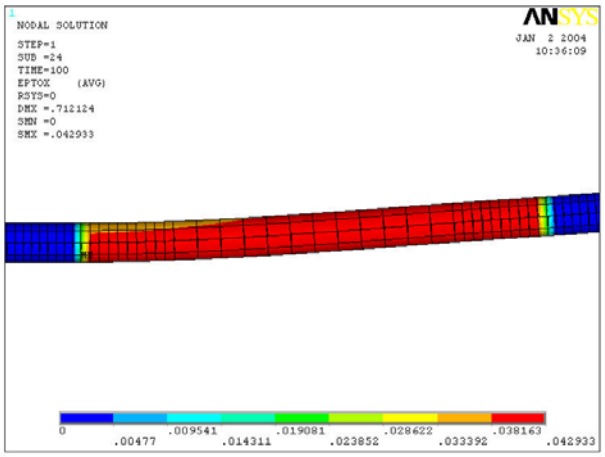

Figure 10 Steel Bar Axial Total Strain Distribution

Table 3 FEA Result

Case Study No.	Average Axial Strain ε_{avg}	Maximum Bending Strain ε_b	$\varepsilon_{total} = \varepsilon_{avg} + \varepsilon_b$	$(\varepsilon_b / \varepsilon_{avg})$ (%)
1	0.0398	0.0035	0.0433	8.8
2	0.0392	0.0038	0.0430	9.7
3	0.0398	0.0025	0.0423	6.2
4	0.0392	0.0026	0.0418	6.7
5	0.0400	0.0029	0.0429	7.2
6	0.0198	0.0019	0.0217	9.5

The above figures show the development of plastic strains in the mild steel bar with its highest value at the fixed end of the bar (Figure 10). The vertical deformation across the unbonded segment of the bar is plotted in Figure 11 for Model No.1and in Figure 12 for all model cases.

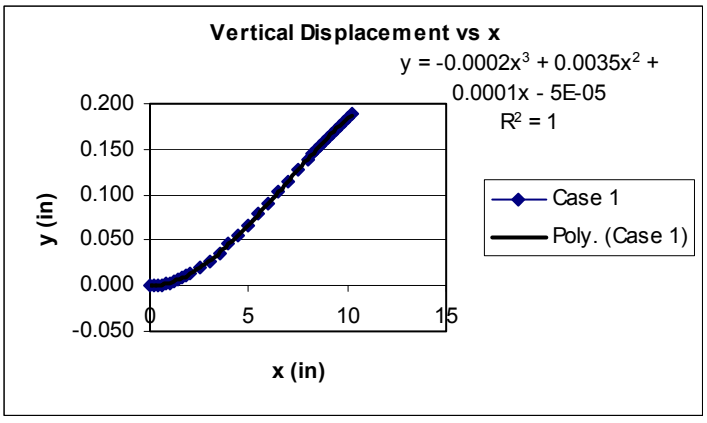

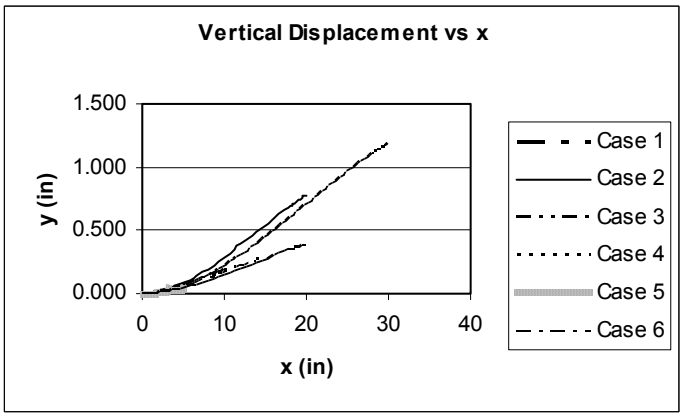

Figure 11: Vertical Deformation of the Unbonded Segment of the Bar
Figure 12: Vertical Deformation of the Unbonded Segment of the Bar

In all six model cases, the vertical deformation data for the bars were fitted into a 3rd order polynomial. The R^2 value of this regression analysis is 1.0 in all cases, which means that the regression results provide perfect fit for the FE results. The equations for the vertical deflection, slope, second derivative, curvature, and bending strain take the following form:

$$y = ax^3 + bx^2 + cx + d \quad (13)$$

$$y' = 3ax^2 + 2bx + c \quad (14)$$

$$y'' = 6ax + 2b \quad (15)$$

$$\Rightarrow \frac{1}{R} = \frac{6ax + 2b}{\left[1 + \left(3ax^2 + 2bx\right)^2\right]^{\frac{3}{2}}} \quad (16)$$

A general equation for the bending strain in the bar can be determined using constants a, b, c, and d based on the prescribed boundary conditions as follows:

Boundary Conditions:

At x = 0

$y = 0 \Rightarrow d = 0$; $y' = 0 \Rightarrow c = 0$

At x = L_{su}

$y = \Delta y$

$y' = \theta_{des} \Rightarrow a = \frac{\theta_{des} L_{su} - 2\Delta y}{L_{su}^{\ 3}}$; $b = \frac{3\Delta y - \theta_{des} L_{su}}{L_{su}^{\ 2}}$

Using Δy and L_{su} values from equations 10 and 8,

$$a = \frac{\left[\theta_{des} - 2(\theta^2_{\ des} + \varepsilon^2_{\ a,a})^{\frac{1}{2}} \sin(\frac{\theta_{des}}{2} + \alpha'')\right]}{\left(\frac{(1 - \eta_{des} - \zeta) h_g \theta_{des}}{\varepsilon_{a,a}}\right)^2} \quad (17)$$

$$b = \frac{\left[3(\theta^2_{\ des} + \varepsilon^2_{\ a,a})^{\frac{1}{2}} \sin(\frac{\theta_{des}}{2} + \alpha'')\right] - \theta_{des}}{\left(\frac{(1 - \eta_{des} - \zeta) h_g \theta_{des}}{\varepsilon_{a,a}}\right)} \quad (18)$$

According to the FE results the values of both the curvature and bending strain are maximum at the fixed end of the bar (at x =0). Therefore:

$$\left(\frac{1}{R}\right)_{\max} = 2b \quad (19)$$

$$and \ \varepsilon_{b,\max} = \frac{d_b}{2}\left(\frac{1}{R}\right)_{\max} = bd_b \quad (20)$$

where $\varepsilon_{b,max}$ is the maximum bending strain along the length of the bar. Substituting for b from Eq. 16,

$$\boldsymbol{\varepsilon_{b,\max} = \left\{\left[3(\theta^2_{\ des} + \varepsilon^2_{\ a,a})^{\frac{1}{2}} \sin(\frac{\theta_{des}}{2} + \alpha'')\right] - \theta_{des}\right\}\left(\frac{d_b}{L_{su}}\right)} \quad (21)$$

REFERENCES

1. ANSYS Theory Manual, version 5.6, 2000
2. Cheok, G.S. and Stone, W.C. (1994). "Performance of 1/3 Scale Model Precast Concrete Beam-Column Connections Subjected to Cyclic Inelastic Loads – Report No. 4". Report No. NISTIR 5436, NIST, Gaithersburg, MD, June.
3. Mander, J.b., and Priestley, M.J., 'Theoretical Stress-Strain Model for Confined Concrete", Journal of Structural Engineering, Vol. 114, No. 8, August, 1988, pp. 1804-1826.
4. Mander, J.B., Panthaki, F.D., a., (1994), "Low-Cycle Fatigue Behavior of Reinforcing Steel,"Journal of Materials in Civil Engineering, ASCE, Vol.6, No.4, pp. 453-468.
5. Chin Liu, Wen, 2001, "Low Cycle Fatigue of A36 Steel Bars Subjected to Bending with Variable Amplitudes", Ph.D Thesis, State University of New York at Buffalo.
6. Hawileh, Rami, 2003, "Non-Linear Finite Element Analysis of Precast Hybrid Beam-Column Connections Subjected to Cyclic Loads", Ph.D Thesis Proposal, University of Wisconsin Milwaukee, Milwaukee, WI.
7. Collins, Jack A., 1993, "Failure of Materials in Mechanical Design: Second Edition", Ohio State University, Columbus, OH.
8. Stanton, John F. and Nakaki, Susan D. (2002). "Design Guidelines for Precast Concrete Seismic Structural Systems", PRESSS Report No. 01/03-09, UW Report No. SM 02-02, Seattle, WA 98195, February